Craze Plasticity in Low Molecular Weight Diluent-Toughened Polystyrene

A. S. ARGON

Department of Mechanical Engineering, Massachussetts Institute of Technology, Cambridge, MA 02139

Received 5 May 1998; accepted 4 August 1998

ABSTRACT: Based on the extensive experiments of Qin et al.[9] on the effects of low molecular weight liquid-rubber diluents on the craze plasticity of polystyrene and the substantial toughening obtainable in certain ranges of temperature, strain rate, and diluent character, we examine in this article the various factors that limit the beneficial toughening effect of such diluents. We find that the principal limitation is the inability of the diluent to keep up with the local plastic deformation process which it affects autocatalytically. A subsidiary limitation is the rate of wetting of the craze borders by the spreading diluent rubber as the latter is released from submicron size diluent pools by the craze itself. While we find it difficult to quantitatively separate in importance the diluent spreading effect from the actual effect of plasticization associated with the autocatalytic sorption of the diluent at the deforming craze borders, the latter appears to be the dominant effect which eventually limits the toughening. © 1999 John Wiley & Sons, Inc. J Appl Polym Sci 72: 13–33, 1999

Keywords: craze plasticity; diluent toughening; solvent crazing

INTRODUCTION

Crazing in flexible chain glassy polymers is a central phenomenon in their mechanical response. It provides the ability for many such polymers to exhibit plasticity in tension in a layered dilatational form which, under certain conditions, can be quite extensive. Crazes, however, are also the precursors to fracture, initiated either from adventitious inclusions entrapped in craze matter, or by tearing of the craze matter itself, initiated from intrinsic irregularities in the latter. In spite of its importance, and in spite of much definitive experimentation and many attempts in modeling, the formation and growth of crazes in flexible chain glassy polymers still remains inadequately understood.[1–4] Recent investigations of the effects of diluents that promote crazing in polystyrene as well as the attendant toughening have focused attention on the fundamental process of craze growth and the self-similar translation of craze borders.These experimental investigations, which we examine briefly in the next section, and their associated modeling studies, have permitted a more detailed look at the fundamental processes of crazing and craze plasticity and the specific role of plasticizing diluents. In this article we present new models to explain some earlier findings.[5–9]

EXPERIMENTAL

Stimulated by the results of the earlier experiments of Gebizlioglu et al.[10,11] on the toughening of PS with diluent modified PS/PB block copolymer particles, additional experiments were per-

---

Correspondence to: A. S. Argon.

Contract grant sponsor: NSF/MRL; contract grant number: DMR-90-22933.

Contract grant sponsor: MRSEC Program of the NSF; contract grant number: DMR-94-00334.

Journal of Applied Polymer Science, Vol. 72, 13–33 (1999)

© 1999 John Wiley & Sons, Inc. CCC 0021-8995/99/010013-21

formed with low molecular weight PB diluents alone in PS, which produced remarkable toughening effects with the incorporation of only 1–2% of those diluents that had precipitated out in a mist of submicron sized pools.[5] Through specific SAXS experiments carried out by Brown et al.[12] on crazed samples of diluent-modified PS it was postulated that the diluent was effective through its autocatalytic plasticizing effect of the craze matter during its formation. A model of this form of toughening through enhanced craze plasticity by Argon et al.[6] had considerable success in accounting for the monotonic reduction of the craze-flow stress at room temperature with increasing volume fractions of precipitated liquid diluent. To verify the findings of that model and test some of the assumptions on the rates of sorption of diluents, new experiments were carried out by Spiegelberg et al.[7,8] to measure wetting and spreading properties of PB diluents on craze borders and the stress dependence of craze velocities in a number of PB diluent-modified blends of PS. Additional experiments on diluent penetration rates into both PS and other model polymers were also conducted by Nealey et al.[13,14] to test the kinetical aspects of the mechanism of craze advance and its dependence on Case II diffusion. Meanwhile, the range of the toughening mechanisms by diluent incorporation itself was studied intensively by Qin et al.[9] which produced much additional information on the temperature and strain-rate dependence of the toughening. All these experiments indicated that the craze-plasticity model of Argon et al.[6] needed reexamination to better understand the limitations of the method of toughening by diluents. In this article, we report new findings, and offer a modified model for such diluent induced effects in craze plasticity.

MODELS FOR DILUENT-ENHANCED CRAZE PLASTICITY

Sources of Rate Dependence in Craze Plasticity of Diluent Modified Blends

In the study of Qin, et al.,[9] the dependence of the craze-flow stress on temperature at a strain rate of 2.6 x 10^{-4}sec^{-1} and on strain rate at room temperature was investigated for a blend with a PB diluent of 3kg/mole molecular weight (PB-3K) having 85% 1,4 content (see Figs.11c and 14b of that study). Moreover, in that same study the dependence of the craze-flow stress at room temperature and a strain rate of 2.6×10^{-4} sec^{-1}on diluent fluidity was also investigated in detail (see Fig. 9 of that study). The effects of these factors, of temperature, strain rate, and diluent fluidity on the toughness could not be explained very well in the context of the previous craze plasticity model of Argon et al.[6] Moreover, the new, detailed, craze-velocity measurements in PS/PB-3K blends, as a function of diluent concentration, carried out by Spiegelberg et al.[7,8]pointed out additional difficulties with the previous model.

Here we start out by identifying two complementary possibilities that must be considered as accounting for the rate dependence. First, the diluent pools that are tapped by an advancing craze, both at its tip and at its widening borders, must spread their contents along the craze border between the craze tufts. The diluent must arrive at the active bases of the craze tufts where tuft drawing proceeds. This diluent spreading will be primarily driven by capillary forces, and its rate will strongly depend on the fluidity of the diluent. This process, which we will analyze in detail, is not likely to be the single source of the rate effects controlling the flow stress or the craze velocity in the small strain rate and higher temperature range where the diluent coverage of the craze surfaces should always be complete. As the strain rate, or craze velocity increases, or the temperature decreases, the diluent coverage becomes partial and will eventually be too incomplete to produce any significant plasticization at the craze borders. The model we present in this article provides a quantitative evaluation of this effect.

Second, is the autocatalytic sorption of the diluent into the plastically deforming base regions of the craze tufts and the associated plasticization that establishes the level of plastic resistance, that controls the actual drawing rate of craze tufts out of the solid polymer. Our model will demonstrate that this process is exceedingly complex, and that it occurs in a zone of high deformation and diluent concentration gradients. The translation of the process front at the base of the craze tuft into the solid polymer must be by a modified Case II sorption process in which the out-of-plane tensile stress acting across the craze border plays a major role. This was pointed out first by Brown[15] in a model attempting to improve on the much quoted Thomas and Windle model[16] which, as we demonstrate in another article, has serious shortcomings.[17] The complexity of this

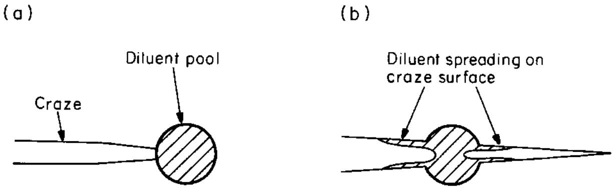

Figure 1 Schematic illustration of a craze tapping into a spherical diluent pool: a) advancing craze tip has tapped into the pool (craze structure is not shown for clarity), b) an intermediate stage of draining of the diluent on the craze borders as the craze tip has advanced further.

drawing process increases through its autocatalytic nature, where, in the actively deforming zone, the sorption is very substantially enhanced by a sharp increase in the diffusion constant through the molecularly-dilated flow structure of the polymer. This phenomenon, which has been suspected by a number of investigators,[14,18,19] has now been experimentally evaluated by Zhou et al.[20] and will be presented elsewhere. Our model, which is presented in this article, shows that these effects are assigned quantitative ranges in space and time where they dominate. However, no attempt is made to deal with the full dimensions of the autocatalytic nature of the sorption, deformation, and plasticization processes that control the drawing. Nevertheless, the model demonstrates a regular behavior pattern and explains how this pattern becomes ineffective in ranges of extreme behavior.

Diluent Spreading on Craze Surfaces

Figures 1a and 1b show the conceptual model of the spreading of liquid diluent onto the surface of a craze as the latter taps into a diluent pool. In Figure 1a, the craze front (craze tufts not shown for clarity) cuts into the spherical pool, while Figure 1b depicts an intermediate stage of spreading of the diluent onto the surface by capillary action after the craze has tapped into the pool. A similar, but somewhat more complex process must occur when the craze border translates laterally and joins into diluent pools. We consider only the case of interaction of the craze front with a typical diluent pool. To evaluate development of this spreading process, measurements of diluent spreading as a function of time were carried out by Spiegelberg et al.,[8] where small droplets of PB-3K diluents with a 71% 1,4 content were placed on clean surfaces of PS, and the change in the radius with time of the spreading diluent slick was recorded. Figures 2a and 2b show the radii of such slicks as a function of time for cases at room temperature and at −20°C respectively (each set of points corresponds to a separate experiment). The rapid early spreading of the slick is due to gravitational forces, while the relatively slower later stages are due to capillary driving forces of interest in our model. Figures 3a and 3b depict the conceptual process of spreading of the diluent droplet (in the Spiegelberg experiment) which is considered to be initially in the shape of a hockey puck of initial height h_o and the initial radius R_o. In Figure 3b the slick is shown in an intermediate state, while Figure 3c depicts the capillary driving forces.

An approximate upper-bound solution of the spreading diluent slick, accounting for viscous

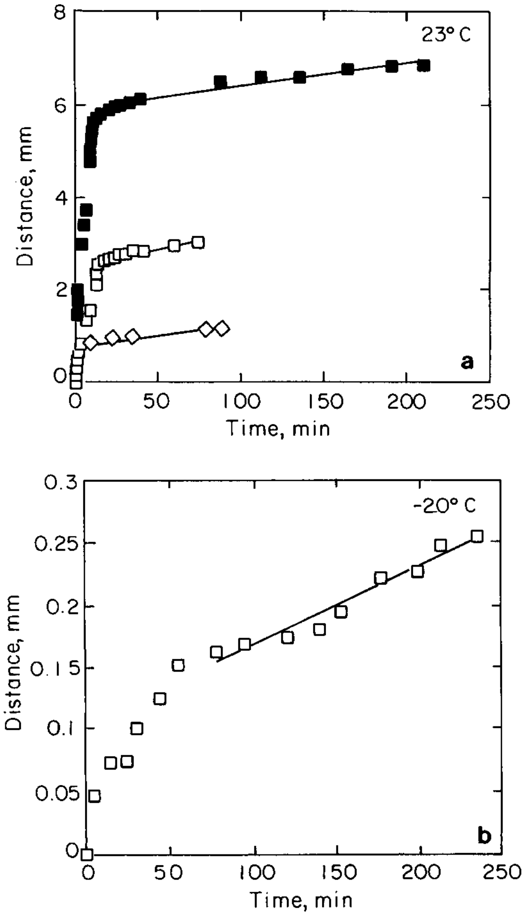

Figure 2 Time dependent spreading of PB-3K diluent droplet with 71% 1,4 content on a PS surface: a) at 23°C, b) at −20°C. The initial radius of the droplet was ca. 1mm (from Spiegelberg et al., Ref. 8, courtesy of J. Appl. Polym. Sci.).

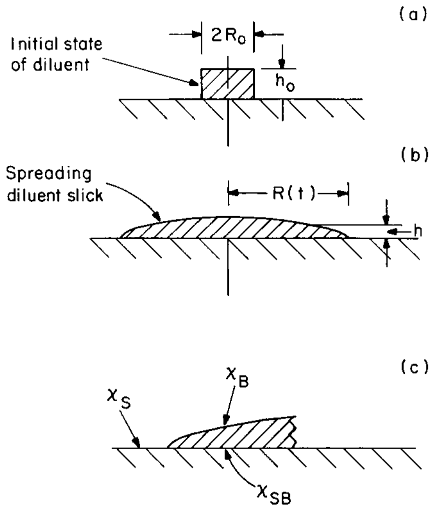

Figure 3 Schematic illustration of the spreading-related-growth of a diluent droplet under the action of capillary forces on a PS surface: a) initial assumed cylindrical shape of droplet, b) an intermediate stage of spreading, c) diluent-droplet front under capillary forces.

dissipation rates, is developed in some detail in Appendix I, and leads to the time-dependent increase of the radius of the slick, *R(t)*, given by the expression below as:

$$\left(\frac{R(t)}{R_o}\right)^4 - 1 = \frac{t}{t_{oc}} \tag{1a}$$

where

$$t_{oc} = \frac{\pi\eta R_o^4}{16V}\,\frac{1}{[\chi_S - (\chi_B + \chi_{SB})]} \tag{1b}$$

and where V is the volume ($=\pi R_o{}^2 h_o = \pi R^2(t)h(t)$), η the extensional flow viscosity of the diluent, χ_s the surface energy of the PS, χ_B that of the diluent PB, and χ_{SB} the interface energy between the diluent and the PS substrate at the appropriate temperatures. The appropriate time normalization constant for spreading under capillary forces is designated as t_{oc}.

The very rapid initial spreading at 20°C shown in Figure 2a is due to gravitational effects. For this range, a different development is appropriate, which gives (Appendix I):

$$\left(\frac{R(t)}{R_o}\right)^2 - 1 = \frac{t}{t_{og}} \tag{2a}$$

where

$$t_{og} = \frac{\eta}{h_o \rho g} = \frac{\eta\pi R_o^2}{\rho g V} \tag{2b}$$

is the relevant time-normalization constant for gravitational spreading.

The data for spreading presented in Figures 2a and 2b is plotted in Figure 4 in two ways. The data at 20°C is plotted according to Eqs.(1a) and (2a) for a diluent droplet of 1mm initial radius, and for an extensional flow viscosity of 20 Pa-s and a capillary factor $[\chi_s-(\chi_B+\chi_{SB})]$ of 0.01J/m^2 as a reasonable estimate resulting in t_{og} = 30.6 sec and in t_{oc}=0.28 sec. The data at −20°C (open diamonds) is plotted only according to the capillary conditions of Eq.(1a) for which the viscosity was adjusted upward according to the (universal) temperature dependence of the viscosity of fluids[21] giving t_{oc} = 84.4 sec at 253K. The results show quite good agreement for the capillary driven spreading at −20%C for all times. On the other hand, gravitational spreading appears to be governing in the short time range of room temperature behavior (open squares). The long-time spreading behavior at room temperature (open squares) departs strongly from the expected capillary behavior. A likely explanation for this is contamination of the diluent over the long periods of observation at room temperature resulting in a gradual increase in viscosity. The relevance of these developments is only to demonstrate that the spreading of the diluent is time dependent and that this will influence the steady state diluent coverage of the craze border where the plastic drawing action is concentrated. On the scale of

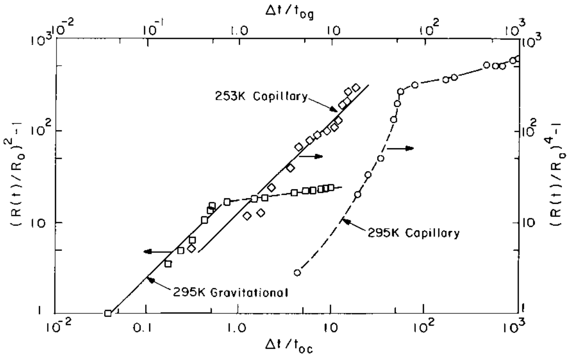

Figure 4 The spreading behavior of PB diluent droplets on PS surfaces plotted against time for both the gravitional spreading conditions and the capillary driving condition at both 295K and 253K.

the craze microstructure we expect that the spreading will be controlled primarily by capillary forces and that Eq.(1a) will govern.

While the role of diluent spreading in craze plasticity must be viewed as a kinetic one in the context of advancing craze fronts, or interfaces, as we will discuss later in this article, it is instructive to determine a full coverage time of spreading of diluent slicks under stationary conditions. If the average diameter of the spherical diluent pools sectioned by the plane of the craze is a then according to the principles of stereology the average radius $\bar{R}$ of the area allocated to each pool on the plane of the cut, will be, for the precipitated diluent fraction of f[6]:

$$\bar{R} = a/2\sqrt{f}. \tag{3}$$

Thus, the average time for complete coverage of the surface of the craze by the diluent in a static situation by the capillary mechanism will be from Eq.(1a).

$$t_f = t_{oc}\left(\frac{1}{4f} - 1\right). \tag{4}$$

Thus, for a PB-3K diluent of 71%1,4 content used by Spiegelberg et al.,[8] the time for full coverage will be about 2 sec. at 295K and 620 sec at 253K for a typical precipitated diluent volume fraction of 0.03 considered by Qin et al.[9] These times, while not quite relevant, provide a crude measure of the limitations of the diluent-toughening mechanism at lower temperatures.

Diluent Coverage of Craze Surfaces during Craze Growth

Here we consider spreading diluent slicks that have been released by the advancing craze front itself to ascertain the conditions of diluent coverage of the craze front. A similar development can be produced for the lateral translation of a widening craze border. We assume that for much of the growth history of a craze, the frontal advance will be linked to the lateral translation of the border by a geometrical relation. Therefore, we will deal with the craze growth and its interaction with diluent pools in one or the other geometry on the basis of whichever is easier to develop.

Figure 5 shows a craze front advancing with a velocity v_c,that has tapped into a diluent pool at a distance v_ct behind the front. At time t the spreading diluent slick covers a length Λ of the craze front, which should be:

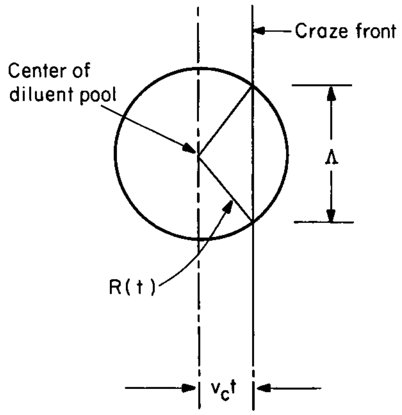

Figure 5 Schematic illustration of a spreading diluent slick tapped-in by a craze front advancing with a velocity v_c. The tapping has occured at a time t before the current position of the craze front, where the diluent wets a length Λ of the front.

$$\Lambda(t) = \sqrt{(2R(t))^2 - (2v_ct)^2}. \tag{5}$$

(The analysis presented is intended to provide only rough magnitudes for effects and employs many approximations such as the overlap between the diluent slick and the solid polymer ahead of the craze front depicted in Fig. 5).

The total time τ that the particular spreading slick can make contact with the advancing craze front is given by:

$$R(\tau) = v_c\tau. \tag{6}$$

This together with Eq.(1a) gives the relation:

$$\left(\frac{v_ct_{oc}}{R_o}\right)^4\left(\frac{\tau}{t_{oc}}\right)^4 - \left(\frac{\tau}{t_{oc}}\right) - 1 = 0, \tag{7}$$

the solution of which provides the required information for τ. In this development we have assumed that the spreading of the diluent is governed by capillary driving forces. Replacing τ with $R_f(=v_c\tau)$, the maximum radius of the spreading slick where contact with the craze front is lost, Eq.(7) can be transformed into one for the terminal radius R_f as:

$$\left(\frac{R_f}{R_o}\right)^4 - \left(\frac{R_o}{v_ct_{oc}}\right)\left(\frac{R_f}{R_o}\right) - 1 = 0. \tag{7a}$$

We examine the typical magnitude of the coefficient of the second term (See Appendix II),

$$\frac{R_o}{v_c t_{oc}} \cong \frac{7\pi}{2}\,\frac{(\chi_S - (\chi_B + \chi_{SB}))}{v_c \eta}\,\lambda_n\left(\frac{d}{h}\right)^2 \qquad (8)$$

where we have replaced the simple extensional flow viscosity with a modification,

$$\eta \rightarrow \frac{2\eta}{\lambda_n}\left(\frac{h}{d}\right)^2 \qquad (9)$$

to take account of the fact that the diluent must spread through craze tufts as a microporous medium in D'arcy-flow fashion, where $\lambda_n$is the average extension ratio of craze tufts h their height (average craze opening displacement) and d the craze tuft diameter. Since, however, the diluent does not fill the craze microstructure, but only wets the borders, $h/d \cong 1.0$ could be taken. For a typical craze front velocity of 10^{-8}m/sec., η in the range of $10-100$ Pa-s, and the capillary factor in the range of 0.01J/m^2, the coefficient of Eq.(8) can be estimated to be of the order of 10^5-10^8. With $R_f/R_o > 1.0$, Eq.(7a) will have a simple solution of,

$$\frac{R_f}{R_o} \cong \left(\frac{R_o}{v_c t_{oc}}\right)^{1/3}. \qquad (10)$$

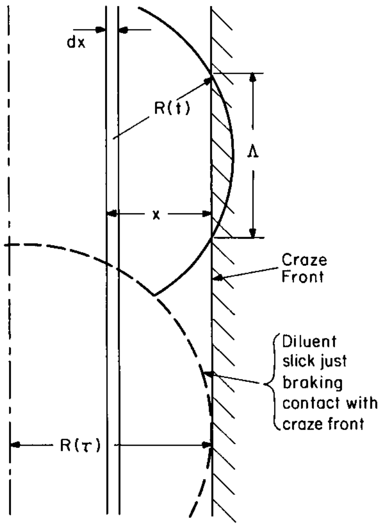

Figure 6 Schematic illustration of two diluent slicks tapped into by the craze front at two earlier times. The lower slick at its extreme range R(τ) has just broken contact with the craze front, while the upper one, tapped into later, still wets a length Λ of the craze front.

To determine the steady-state coverage of the craze front with diluent, the interaction of the front with all possible spreading diluent slicks must be considered. To do this, we integrate the contributions of all spreading slicks previously tapped by the advancing front, as depicted in Figure 6. The craze front will receive contributions from a number dn per unit length, of pools located in a strip of width dx behind the craze front at position x, where,

$$dn = N dx \qquad (11)$$

and

$$N = \frac{64f}{\pi^3 a^2} = \frac{R_o^2 f}{\pi} \qquad (12)$$

is the number density of intercepted pools by the craze plane for pools of diameter a and making up a volume fraction of f . Since each pool at a distance x behind the front provides a coverage length of Λ, the total line fraction c of the craze front covered by diluent reaching the front from behind will be,

$$c = \int_0^{x=R_f} \Lambda(x) N dx$$

$$= \frac{R_o^2 f}{\pi}\int_0^{Rf} \sqrt{(2R_o)^2\left(1 + \frac{x}{v_c t_{oc}}\right)^{1/2} - (2x)^2}\,dx \qquad (13)$$

where R_f is given by Eq.10. Taking advantage of a number of simplifications, explained in Appendix II, the steady state line fraction of the craze front covered by diluent for a front advancing with a velocity v_c becomes,

$$c \cong \pi\beta f\left(\frac{\lambda_n(\chi_S - (\chi_B + \chi_{SB}))}{v_c \eta}\left(\frac{d}{h}\right)^2\right)^{2/3} \qquad (14)$$

where

$$\beta = \int_0^1 \sqrt{\xi^{1/2} - \xi^2}\,d\xi = 0.561 \qquad (15)$$

is a definite integral.

While Eq.(14) itself is informative, a further modification will be even more useful. Considering the craze strain rate to be the result of a steady state density ρ of active craze front length per unit volume, where each craze produces an inelastic opening displacement b as the fronts advance with a velocity v_c,i.e.,

$$\dot{\epsilon}_c = b\rho v_c, \tag{16}$$

it is possible to replace v_c with the associated strain rate $\dot{\epsilon}$ to obtain:

$$c = \pi\beta f\left(\frac{(\chi_S - (\chi_B + \chi_{SB}))\lambda_n(b\rho)}{\dot{\epsilon}_c\eta}\left(\frac{d}{h}\right)^2\right)^{2/3}. \tag{17}$$

From the Spiegelberg et al.[8] measurements it is possible to estimate $bp \approx 0(2.6 \times 10^4 m^{-1})$. Then taking $\lambda_n = 4.0, f = 0.03$, $\eta = 10\text{Pa}-s$, $d/h \approx 1.0$, $\beta = 0.561$, we estimate the critical strain rate where the coverage becomes less than unity to be $\dot{\epsilon}_c = 1.26\ sec^{-1}$ at room temperature for the diluent used by Spiegelberg et al.[8] We note that for a less fluid diluent with a PB 1,4 fraction at only 0.16 (η = 100 Pa−), $\dot{\epsilon}_{cc} = 0.126$, and for a more fluid one with PB 1,4 fraction at 0.85 (η = 2 Pa−s), $\dot{\epsilon} = 6.32\ \text{sec}^{-1}$ respectively. Comparing these critical strain rates with those observed by Qin et al.[9] for the above blends when significant reductions in toughening set-in at smaller strain rates, we must conclude that while the diluent spreading kinetics is important, it is not likely to be the main factor that governs the toughness response. A factor of at least as much importance is the actual kinetics of the complex local autocatalytic sorption, plasticization, and plastic drawing process at the deforming bases of the craze tufts which we present in the next section.

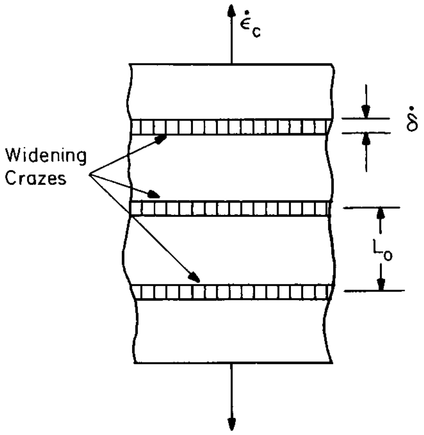

Figure 7 An idealization of craze plasticity where the tensile-craze strain rate $\dot{\epsilon}_c$ is fully accounted for by the thickening rate $\dot{\delta}$ of crazes at average spacing L_o.

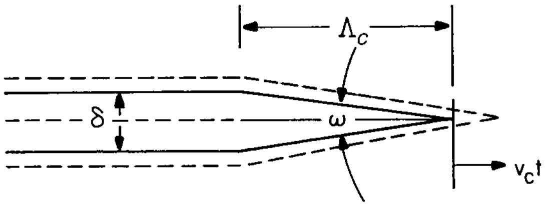

Figure 8 Schematic illustration of the relationship between the forward advance rate of a craze with velocity v_c and the thickening rate $\dot{\delta}$ of the craze, through an assumed craze-tip dart angle ω over a characteristic length Λ_c.

Parenthetically, we observe again that the above considerations for diluent coverage based on the advance of the craze front should also apply, to within a constant factor of proportionality, to craze borders receding laterally.

Model for Craze-Flow Stress and Craze Velocity in Diluent-Plasticized Blends

Intrinsic Response of the Homopolymer

In craze plasticity the overall tensile strain rate, in fully developed flow, is kinematically related to the lateral translation of a given volume density of active craze borders as depicted in Figure 7, where the overall tensile strain rate $\dot{\epsilon}_c$ can be considered to arise from the thickening rate $\dot{\delta}$ of active planar crazes at an average spacing of L_o, i.e.:

$$\dot{\epsilon}_c = \frac{\dot{\delta}}{L_o}. \tag{18}$$

A complementary view concentrating on the rate of longitudinal growth of crazes was that given by Eq.(16) where v_c is the growth rate of crazes which is far easier to measure than the associated thickening rate $\dot{\delta}$ cited above. We assume that the two alternative forms of representation are geometrically linked through a characteristic craze tip "dart" having a tip angle ω as shown in Figure 8. The two forms of representation would then be linked through the geometrical relation:

$$v_c = \frac{\dot{\delta}}{\omega}, \tag{19}$$

giving moreover,

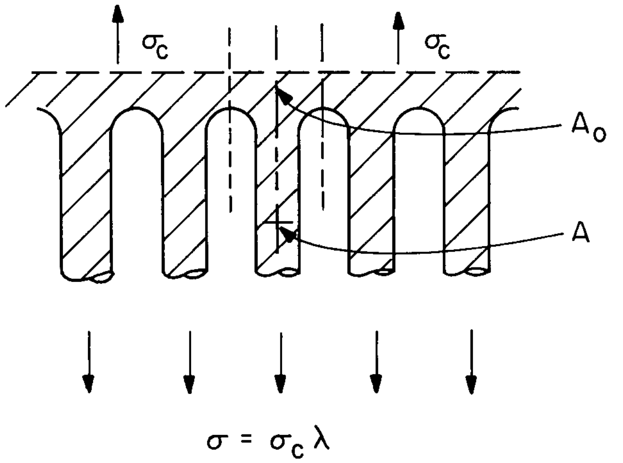

Figure 9 The idealized model of a craze border where periodically placed tufts are being drawn out under the prevailing craze stress σ_c. To a first approximation, the outlined tuft will be considered as if it were the shoulder region of a propagating neck in a tensile bar.

$$b\rho = \frac{\omega}{L_o}, \qquad (20)$$

where the interpretation of $b\rho$ was given in connection with Eq.(16) above.

Since the plasticizing effect of the diluents is best understood at the action sites along the translating craze borders, we develop our model for the craze-flow stress on the basis of the representations depicted in Figure 7, but relate the development to the craze velocity through Eq.(19).

Figure 9 shows an idealized representation of the border region of a craze composed of a series of tufts being drawn out from the solid polymer under a craze-flow stress of σ_c to an eventual extension ratio of λ_n. While there are important differences, the local action can be viewed as what goes on at the shoulder regions of a tension bar as depicted in Figure 10, where the drawing velocity v_d is related to the velocity c_d of translation of the shoulder through:

$$v_d = c_d(\lambda_n - 1). \qquad (21)$$

The mechanics of this problem has been considered by Hutchinson and Neale[22] as a steady state drawing process and by Boyce et al.[23] in considerable detail, concentrating on the shoulder region where the drawing action occurs. The simulation of Boyce et al. shows that the elongation rate $d\epsilon_o/dt$ of the stretching bar, where the elongation is a result of two shoulders travelling apart with velocities c_d along the bar, the deformation is concentrated in the narrow shoulder regions where all the action occurs at an equivalent local plastic strain rate of:

$$\dot{\epsilon}_e^p = \beta\,\frac{d\epsilon_o}{dt} = \beta\,\frac{1}{2R}\,v_d = \beta\,\frac{1}{2R}\,c_d(\lambda_n - 1). \qquad (22)$$

The level contours of local concentrated equivalent plastic strain rates determined by the simulation of Boyce et al. are given in Figures 11a and 11b for two elongation rates $\dot{\epsilon}_o$ of 10^{-2} $\sec^{-1}$ and 10^{2} $\sec^{-1}$ respectively. Over this range of increase of the elongation rate by a factor of 10^4 the local strain rate concentration β averaged across the cross section increases from close to 2 to about 4. Thus, we obtain:

$$c_d = \frac{2R}{\beta}\,\frac{\dot{\epsilon}_o}{(\lambda_n - 1)}, \qquad (23)$$

and a craze thickening rate of

$$\dot{\delta} = 2v_d = 2(\lambda_n - 1)c_d = \frac{4R}{\beta}\,\dot{\epsilon}_e^p, \qquad (24)$$

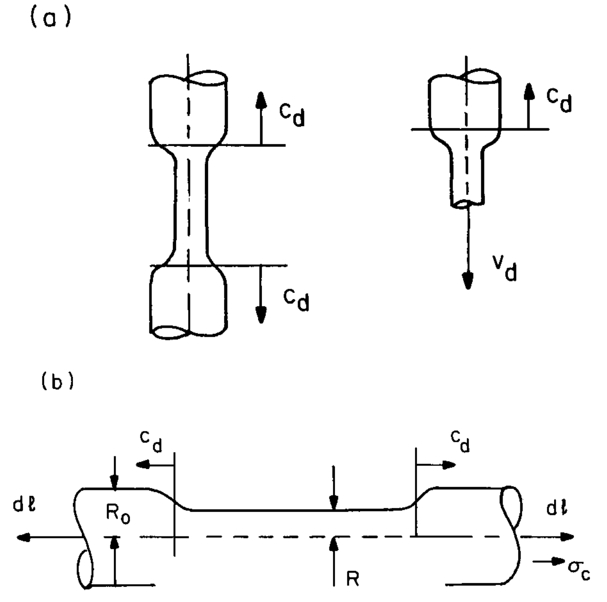

Figure 10 The propagating shoulder of a necked tensile bar as the model for tuft drawing: a) downward velocity v_d of the drawing bar, related to the velocities c_d of propagation of two shoulders of the extending neck (Eq. 21), b) increments of length dl resulting from propagation of two shoulders where, by geometry $2\dot{l} = \dot{\delta}$.

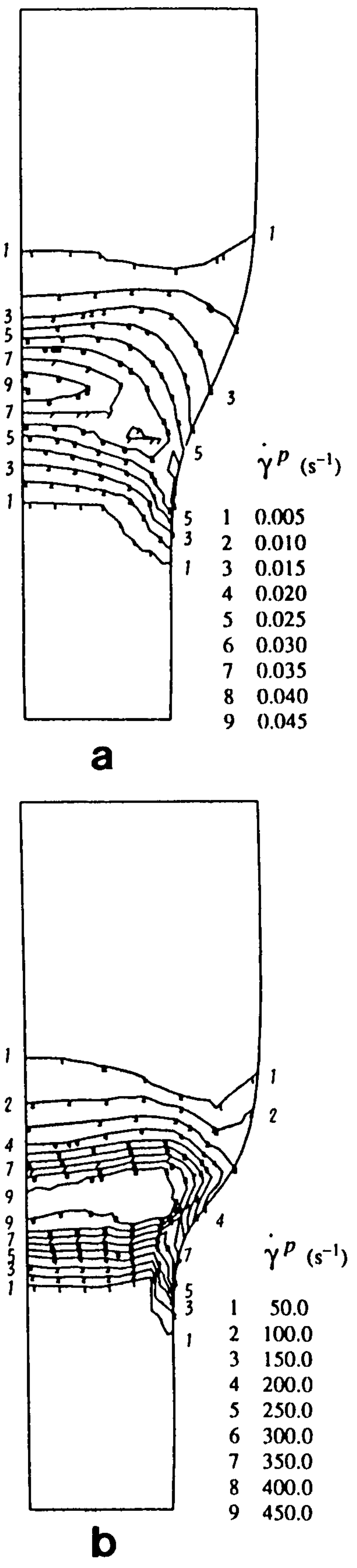

where $\dot{\epsilon}_e^p$ is the local equivalent plastic strain rate averaged across the deforming base zone of the craze tuft. For the dependence of this plastic strain rate on equivalent stress and temperature we use the functional form developed by Argon and Bessonov[24] (AB) based on mechanism-inspired phenomenology, and with it construct the required expression for the craze strain rate $\dot{\epsilon}_c$ using Eqs.(18) and (24).

$$\dot{\epsilon}_c = \frac{2d}{\beta L_o}\,\dot{\epsilon}_{AB}\exp\left[-\frac{B}{RT}\left(1-\left(\frac{\lambda'\sigma_c}{\hat{Y}_o}\right)^{5/6}\right)\right], \quad (25)$$

where $d(=2R)$ is the craze tuft diameter $\dot{\epsilon}_{AB}(=3 \times 10^{12} sec^{-1})$ is the fundamental frequency factor in the AB model, B is an activation free energy with considerable segmental mechanistic detail of little interest here, σ_c the craze flow stress, $\lambda'(=A_o/A)$ the local extension ratio where the drawing action is concentrated, and $\hat{Y}_o$ the athermal tensile plastic resistance. The other terms, β and L_o, have the meanings discussed above, and RT has its usual meaning. In the interface convolution model of craze matter production (on which Eq.(25) is based), the craze tuft diameter is known to relate to the craze-flow stress through the expression:

$$d = \frac{C}{\sigma_c}, \quad (26)$$

where the proportionality constant C is 2.5×10^{-7} MPa$-$m as determined by Brown et al.,[12] Eq.(25) becomes:

$$\dot{\epsilon}_c = \frac{2C\dot{\epsilon}_{AB}}{\beta L_o \hat{Y}_o}\exp\left[-\frac{B}{RT}\left(1-\left(\frac{\lambda'\sigma_c}{\hat{Y}_o}\right)^{5/6}\right)\right]. \quad (25a)$$

The associated craze tip velocity v_c can then be obtained immediately through Eq.(19) as:

$$v_c = \frac{2C\dot{\epsilon}_{AB}}{\beta\omega\hat{Y}_o(\sigma_c/\hat{Y}_o)}\exp\left[-\frac{B}{RT}\left(1-\left(\frac{\lambda'\sigma_c}{\hat{Y}_o}\right)^{5/6}\right)\right]. \quad (27)$$

Figure 11 Distribution of equivalent plastic strain rate in the active shoulder regions of a necked tension bar for two very different elongation rates: a) 10^{-2}sec^{-1}, and b) 10^2 sec^{-1} in the necking model of Boyce et al.[23] of a glassy polymer bar (from Boyce et al., Ref. 23, courtesy of Polym. Eng. Sci.).

where ω is the craze tip "dart" angle to be determined as a fitting constant. Equations (25a) and (27) give expressions for the craze strain rate and the craze -tip velocity in the intrinsic behavior of the unmodified homopolymer.

Effect of Diluent Modification in the Craze-Flow Response

Extensive, new investigations of diluent effects on the toughening mechanism discovered by Gebizlioglu et al.,[5] carried out by Qin et al.,[9] new considerations of Case II sorption[13,14,17] plasticization effects of diluents,[8,15,17]and flow-induced autocatalytic enhancement of diffusion[20] have all stimulated a thorough reexamination of the previous model of Argon et al.[6] In that model it was assumed that diluent penetration into the craze tufts is governed by a sudden increase in local solubility of the diluent in the homopolymer through the deformation-induced negative pressure all along the stem and the base of the craze tuft. This was then assumed to result in nearly "instantaneous" sorption of diluent and material plasticization which defines a significantly reduced local plastic resistance of craze tufts. Experiments of Nealey et al.,[13,14] however, demonstrated that neither the Fickian diffusion nor any Case II sorption can be fast enough to complete the sorption before the plastic drawing takes place in the above assumed manner, and that the sorption and drawing must be concurrent and autocatalytic. Moreover, the above cited new experiments also demonstrated that pressures or negative pressures of up to 40% of the yield stress in the plane of the surface had no measurable influence on the rate of sorption of the diluent. Our new studies, introducing features of concurrent processes into the model, demonstrated that the previous assumptions survived, but the process scenario needed substantial reinterpretation.

In our present model we recognize that, as Figures 11a and 11b demonstrate, the entire action of plasticity that governs crazing response is concentrated in a narrow zone at the base of the craze tuft where deformation gradients and diluent concentration gradients must be very steep. Our present idealization is depicted in Figure 12. Diluent is sorbed into the intensely deforming zone between contours 2 and 3 in an accelerated fashion due to the substantial enhancement of diluent diffusivity, which results from a flow-induced molecular level dilation, or transient production of free volume. New experiments of Zhou et al. have furnished strong evidence for this accelerated diffusion.[20] This produces, in the zone between contours 2 and 3, a steady-state diluent concentration ϕ_e. The diluent concentration is envisioned to produce directed sorption into the interior through the action of a Case II sorption front located primarily along contour 4, where the presence of the tensile stress acting on the craze tufts very substantially accelerates the advance of the front, as proposed by Brown,[15] but by a process quite different in detail from the Thomas and Windle model as we present elsewhere.[17] Nevertheless, for our model to work in the way to be developed below, it is essential that the Case II sorption front precede the advance of the concentrated deformation zone, albeit by perhaps no

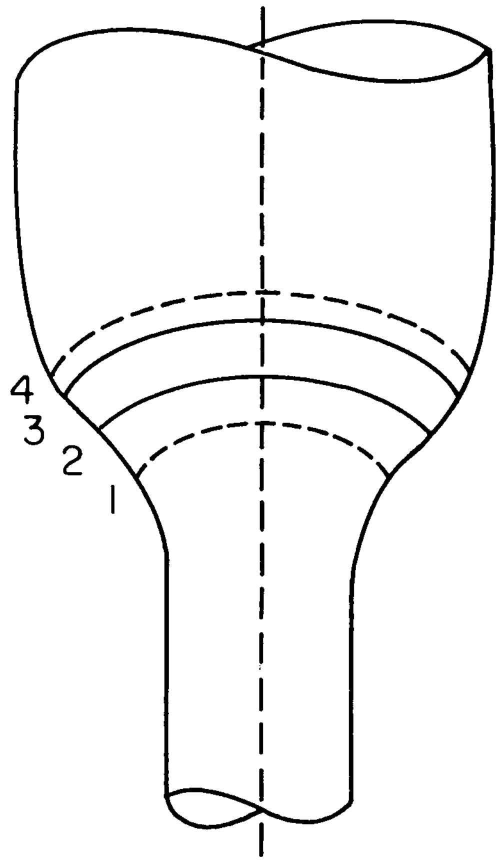

FIGURE 12 Schematic illustration of the various action zones along the base of the actively drawing craze tuft. All action is concentrated into the zone between 1–4. In zone 2–3, an equilibrium diluent concentration φ_e is assumed to have been established. In zones 1–3 deformation and sorption are autocatalytically interacting. The Case II sorption front is assumed to be along contour 4, preceding the active deformation front.

more than a small fraction of the tuft diameter. In addition, the diluent at concentration φ_e will also result in substantial plasticization, and will promote continued drawing in the material zone between 3 and 1. Clearly, the process of deformation-accelerated sorption, plasticization, and drawing out of polymer in the zone between 3 and 1 must be highly interactive or "autocatalytic". The relatively successful nature of the model might be taken as being in support of the above scenario. Eventually, however, at high strain rate, low temperature, or with diluents of high viscosity, the flow stress rises too much and the toughening effect is compromised. This is likely to be due to a combination of threshold effects such as inadequate diluent coverage of the craze surfaces, or the ability of the sorption front (4) to precede the deformation zone (1–3). We examine this possibility more precisely in this article.

If diluent coverage of the craze borders is complete, the free-liquid diluent of volume fraction f released from tapped pools of diameter a, will cover the craze border with a layer of thickness[6]

$$h = \frac{16af}{3\pi^2}. \tag{28}$$

Then over an area $\pi d^2\lambda/4$, allocated to a single craze tuft, the total volume of diluent available per tuft would be

$$V = \frac{16af}{3\pi^2}\,\lambda\,\frac{\pi d^2}{4}. \tag{29}$$

If this available diluent is sorbed into a volume of $\pi d^2\lambda\alpha d/4$, corresponding to the zone between 2 and 3 in Figure 12, where (αd) represents a measure of the thickness of this zone, the volume fraction of diluent φ_e in the zone would be

$$\varphi_e = \frac{16af}{3\pi^2\alpha d}, \tag{30}$$

and with the use of Eq.(26),

$$\varphi_e = \frac{16}{3\pi^2}\,\frac{af\hat{Y}_o}{\alpha C}\left(\frac{\sigma_c}{\hat{Y}_o}\right). \tag{30a}$$

We note that the diluent concentration φ_e is not a result of equilibrium considerations of solubility governed by temperature and pressure (stress), but is governed by availability of diluent, with the assumption that its establishment is rapid, and importantly aided by the transient increase in diffusivity resulting from the flow induced dilations referred to above.[20]

Finally, the principal effect of the sorbed diluent will be plasticization of the base region of the craze tuft. This we express, as before, by stating that the reference athermal plastic resistance would be modified, where $\hat{Y}_o$ becomes replaced by,

$$\hat{Y}_o \;\to\; \hat{Y}_o\exp(-\,m_p\varphi_e), \tag{31}$$

where m_p is the plasticization factor.

With this principal modification, the craze-strain rate $\dot{\epsilon}_c$ and the craze-tip velocity v_c in the diluent modified blend would become,

$$\begin{aligned}\dot{\epsilon}_c = \frac{2C\dot{\epsilon}_{AB}}{\beta L_o\hat{Y}_o(\sigma_c/\hat{Y}_o)}\exp\Bigg[-\frac{B}{RT}\Bigg(1-\Bigg(\frac{\lambda'\sigma_c}{\hat{Y}_o}\Bigg)^{5/6}\\ \times\exp\Bigg(\frac{5m_p}{6}\Bigg)\Bigg(\frac{16}{3\pi^2}\Bigg)\frac{af\hat{Y}_o}{\alpha C}\Bigg(\frac{\sigma_c}{\hat{Y}_o}\Bigg)\Bigg)\Bigg)\Bigg]\end{aligned} \tag{32}$$

$$\begin{aligned}v_c = \frac{2C\dot{\epsilon}_{AB}}{\beta\omega\hat{Y}_o(\sigma_c/\hat{Y}_o)}\exp\Bigg[-\frac{B}{RT}\Bigg(1-\Bigg(\frac{\lambda'\sigma_c}{\hat{Y}_o}\Bigg)^{5/6}\\ \times\exp\Bigg(\frac{5m_p}{6}\Bigg)\Bigg(\frac{16}{3\pi^2}\Bigg)\frac{af\hat{Y}_o}{\alpha C}\Bigg(\frac{\sigma_c}{\hat{Y}_o}\Bigg)\Bigg)\Bigg)\Bigg].\end{aligned} \tag{33}$$

Provided the dynamic coverage of the diluent on the craze borders remains the same, the above expressions should represent steady state values.

Introducing an abbreviation,

$$\dot{\epsilon}_{co} = \frac{2C\dot{\epsilon}_{AB}}{\beta L_o\hat{Y}_o}, \tag{34}$$

we note that the craze flow stress σ_c can then be obtained by determining for a given imposed strain rate $\dot{\epsilon}_c$ and other relevant parameters by solving Eq.(32). This we respresent symbolically as,

$$\frac{\sigma_c}{\hat{Y}_o} = g^{-1}\left(\frac{\dot{\epsilon}_c}{\dot{\epsilon}_{co}}\right), \tag{35}$$

where

$$\begin{aligned}g = \Bigg(\frac{\hat{Y}_o}{\sigma_c}\Bigg)\exp\Bigg[-\frac{B}{RT}\Bigg(1-\Bigg(\frac{\lambda'\sigma_c}{\hat{Y}_o}\Bigg)^{5/6}\\ \times\exp\Bigg(\frac{5m_p}{6}\Bigg)\Bigg(\frac{16}{3\pi^2}\Bigg)\frac{af\hat{Y}_o}{\alpha C}\Bigg(\frac{\sigma_c}{\hat{Y}_o}\Bigg)\Bigg)\Bigg)\Bigg]\end{aligned} \tag{36}$$

and Eq.(35) indicates an operational inversion.

COMPARISON WITH EXPERIMENTS

Evaluation of Parameters

Since the model presented above is not obtainable from first principles, the relevant parameters such as the activation free energy, B, the parameter, λ', the plasticization coefficients, m_p, the craze-tip dart angle ω, and the like, must be determined from a chosen set of experiments which can then be considered as reference experiments to check the predictive capability of the model with regard to the remaining experiments.

We start by fixing B and λ' from the intrinsic craze-plasticity experiments of Spiegelberg et al.[8] for pure PS. For this we take the measured dependence of v_c, the craze velocity, on $\sigma_c/\hat{Y}_o$, the normalized craze-flow stress, at 295K. We take $\hat{Y}_o$ as defined in Ref. 6, to be 238MPa, and as determined from the previous model. Eq.(27) gives,

$$\frac{d\ln v_c}{d(\sigma_c/\hat{Y}_o)} = \frac{B}{RT}\left(\frac{5}{6}\right)(\lambda')^{5/6}\frac{1}{(\sigma_c/\hat{Y}_o)^{1/6}} - \frac{1}{(\sigma_c/\hat{Y}_o)} = 3.83 \quad (37)$$

Choosing a craze-flow stress of $\sigma_c = 30$MPa, from mid range, we obtain,

$$B(\lambda')^{5/6} = 23.0 \text{ kcal/mol.} \quad (38)$$

Proceeding, we take the strain-rate expression of Eq.(25a) and use the above value in Eq.(38), together with the measured peak craze-flow stress of 42MPa at a strain rate of $\dot{\epsilon}_c = 2.6 \times 10^{-4}$ sec^{-1},to solve for B, with the additional parameters of $L_o = 2 \times 10^{-6}$m, $C = 2.5 \times 10^{-7}$ MPa − m, $\dot{\epsilon}_{AB} = 3 \times 10^{12}$sec^{-1} and $\beta = 2.0$, based on information from micrographs of crazes, SAXS measurements, and the model of Argon and Bessonov,[24] to obtain,

$$B = 23.7 \text{ kcal/mol.} \quad (38a)$$

and

$$\lambda' = 0.967 \approx 1.0. \quad (38b)$$

With the above information we determine next, from the craze-velocity expression, the craze-tip dart angle ω as,

$$\frac{1}{\omega} = \frac{v_c\hat{Y}_o}{C\dot{\epsilon}_{AB}}\left(\frac{\sigma_c}{\hat{Y}_o}\right)\exp\left[\frac{B}{RT}\left(1 - (\sigma_c/\hat{Y}_o)^{5/6}\right)\right], \quad (39)$$

where a direct evaluation for a mid range stress of $\sigma_c = 30$MPa gives,

$$\omega = 3.0 \times 10^{-2}. \quad (40)$$

In their experiments on the toughening effect of diluents Qin et al.[9] explored 4 separate diluent blends of PB-3K differing in their viscosities by more than a factor of 100, where the difference resulted from the different 1,4 content of the PB, with the viscosity decreasing sharply with increasing 1,4 content (See Fig. 10a in Ref. 9). The effect of these different diluents, all at the same molecular weight, are shown in Figure 9 of Ref.(9) at room temperature. The changes in the flow stresses for a given reference strain rate of 2.6 × 10^{-4} sec^{-1} is dramatic. We use the measured craze-flow stresses for these blends, as summarized in Table I below, to determine through Eq.(32), the plasticization factors m_p for these blends through the expression,

$$m_p = \frac{1}{\varphi_e}\left[\frac{6}{5}\ln\left(1 + \frac{RT}{B}\ln\left(\frac{\dot{\epsilon}_c L_o\hat{Y}_o}{\dot{\epsilon}_{AB}C} \times \left(\frac{\sigma_c}{\hat{Y}_o}\right)\right)\right) - \ln\left(\frac{\sigma_c}{\hat{Y}_o}\right)\right] \quad (41)$$

where φ_e was given by Eq.(30a). The factors m_p determined in this manner are given in Table I together with other relevant information on these blends in which $f = 0.03$ for all cases.

The Craze Flow Stress

With the parameters determined in the preceding section, we proceed with the type of operational inversion of the craze-strain rate expression discussed previously for the 4 diluent blends used in the recent study of Qin et al.,[9] making use of the plasticization factors m_p listed in Table II. The resulting dependences on liquid diluent content f of the craze-flow stresses at 295K at a strain rate of 2.6 × 10^{-4} sec^{-1} are given in Figure 13 with the solid curves. The flow stress measurements of Spiegelberg et al.[8] for the blend with 71% PB 1,4

Table I Properties of PB-3K Diluents at Volume Fraction f = 0.03 in the Craze Plasticity of the PS/PB-3K Blends Shown in Fig. 13. (T = 295 K, $\dot{\epsilon}_c = 2.6 \times 10^{-4}\ \mathrm{sec}^{-1}$, $\hat{Y}_o$ = 238 MPa)

Microstructure of Diluent (% PB 1,4 fraction)	σ_c (MPa)	$\sigma_c/\hat{Y}_o$	φ_e	Shear Viscosity (Pa-s)	m_p
16	26.9	0.113	0.1743	174.30	2.02
71	24.4	0.102	0.1581	16.10	2.76
74	20.2	0.085	0.1309	10.83	4.57
85	10.6	0.044	0.0687	1.08	16.73

content, shown as the circular data points, agree very well with the predicted dependence. The data points, shown by diamonds relate to the earlier measurements of Gebizlioglu et al.[5] for a very fluid diluent PB-3K which was close to one with a PB-3K 1,4 content of 85%. The agreement of the experiments with the model predictions is good for high diluent content but not very good at the solubility limit. The previous model,[6] which had a number of adjustable parameters could be made to fit the latter experimental data at room temperature much better. Since with our present model the intent is to explore wider ranges of validity over different strain rates and temperatures, and since we have reservations on the structure of the Thomas and Windle[16] model, that inspired our earlier model, we accept our new model in its present form but provide reasons for its breakdown in the extreme ranges of high strain rate and low temperature, as discussed in this article.

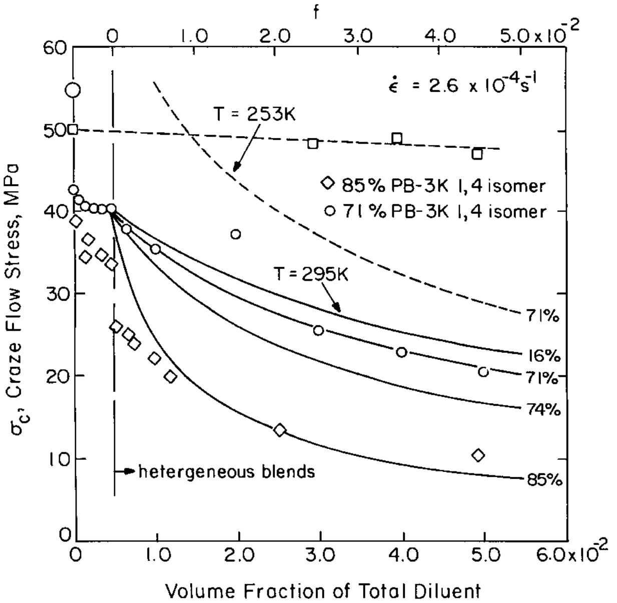

Figure 13 Dependence of the calculated craze flow stresses on volume fraction of diluent at a strain rate of $2.6 \times 10^{-4}\ \mathrm{sec}^{-1}$ and at 295K and 253K for several different PB-3K diluents with different molecular microstructures. The flow stress increases markedly with decreasing 1,4 fraction in the diluent for all volume fractions.

Using the model of Eq.(32) and the same operational inversion procedure implied in Eqs.(35) and (36), we calculate the diluent concentration dependence of the flow stress at T = 253K for a diluent of 71% PB 1,4 content using the same coefficients established previously in this article (keeping the plasticization factor m_p also constant at the value given in Table I). The result is the broken curve in Figure 13. (Since $\hat{Y}_o$ scales with the temperature dependence of the shear modulus, in the conversion of the computed normalized craze-flow stress values $\sigma_c/\hat{Y}_o$, a properly scaled-up value of $\hat{Y}_o$ = 263MPa was used in the plot of Figure 13). The corresponding experimentally measured points by Spiegelberg et al.,[8] given as squares are shown going through a flow-stress level of 50MPa and showing no dependence on diluent content. Moreover, the calculated craze-flow stress of the homo-PS based on Eq.(25a) obtained as 55MPa is shown as the circle on the ordinate axis. Clearly, the broken curve, if properly constructed, should have gone through this point (projected to f = 0). That this is not so, indicates that there are other important temperature-dependent changes in the parameters calculated previously, such as the craze-tip dart angle ω and the plasticization factor m_p, with the latter being the most important. An adjustment of this factor would have satisfied the intercept requirement for the broken curve but would have produced no better agreement with the experimental points. The fact that all the experimental points lie below the projected craze-flow stress of the homo-PS and that there is no important de-

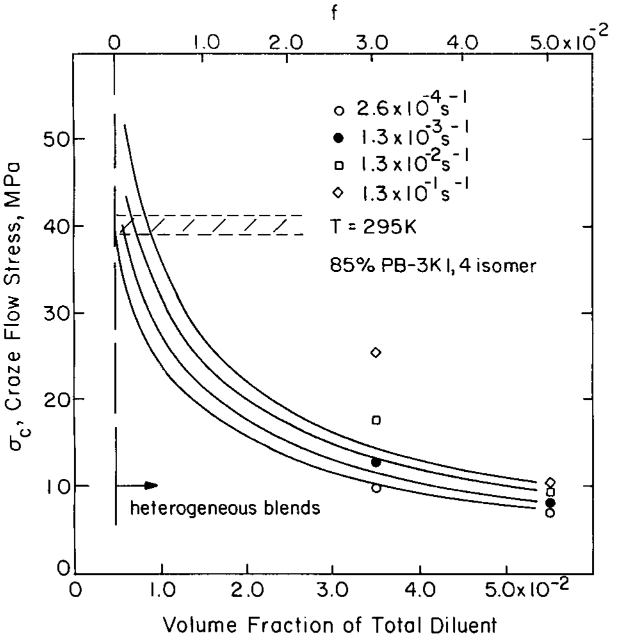

Figure 14 Dependence of the calculated craze flow stresses on diluent volume fraction at 295K but for different strain rates for a diluent with the highest fluidity. The lowest curve for the base strain rate of 2.6 × 10^{-4} $\sec^{-1}$ was used for a basis of adjustment.

pendence of σ_c on diluent content indicates that the diluent is entirely ineffective at this temperature. This is supported by the observations that under these conditions the fractures are brittle and the tensile toughness is no better than that of homo-PS. Later in this article we demonstrate that under these conditions the principal assumption that the Case II sorption front preceded the concentrated deformation zone breaks down, and there is no significant autocatalytic interaction between, sorption, plasticization, and deformation.

Next we explore the effect of imposed strain rate on the craze-flow stress at room temperature as a function of free-diluent concentration *f* for only the most fluid diluent containing 85% 1,4 fraction with diluent plasticization characteristics given in Table I. The resulting curves for four separate tensile-strain rates are given in Figure 14. The lowest curve is the same as the lowest curve for 295K given in Figure 13. To obtain these curves, Eq. (32) was used in which the strain rate was equated to the four different imposed rates followed by solving for $\sigma_c/\hat{Y}_o$. The available data point for a PB-3K volume fraction of the diluent *f* = 0.03 agrees very well with the lowest curve since that was used as the matching condition to determine the various coefficients in this article.The experimental points for the flow stress for other strain rates are all well above the respective curves. This must indicate a systematic breakdown of the diluent coverage condition discussed above, and perhaps also the assumption that the sorption front always precedes the front of intense plastic drawing. The fact that these effects must be present could already be seen from the systematic reductions in tensile toughness with increasing strain rate for all diluent blends studied by Qin et al..[9] The hatched zone at around 40MPa is where fracture occurs in homo-PS with little energy absorption, i.e., where the first few crazes result in fracture. The experimental flow-stress measurements indicate that higher-diluent concentrations are required to avoid brittle behavior at higher strain rate conditions than the model of full autocatalytic interaction would predict.

Craze Velocity-Stress Relationships

Using Eq.(33), we explore next, the dependence of craze velocity v_c on stress for blends with different prepackaged diluent concentrations *f*, but all for the PB diluent with 71% 1,4 fraction, making use of the information on Table I for this diluent blend and the various physical parameter values evaluated above. The results for 295K and 253K are given in Figures 15 and 16 which show the computed results as the light-solid curves for homo-PS (□), for total diluent concentration of 0.01 (*f* = 0.005), (△), for total diluent concentration of 0.03 (*f* = 0.025) (◇) and for total diluent concentration of 0.05 (*f* = 0.045) (○). The corresponding experimental results based on measurements of Spiegelberg et al.[7,8] are shown by the blackened data points of the same shape for these diluent concentrations. The best fit to the experimental results is given for these different diluent concentrations with the heavy solid curves. In Figure 15 there is a good match between the experimental and theoretical behavior patterns for homo-PS (the lowest curves). For higher diluent concentrations there are systematic departures between the experimental values and the theoretical model for given stress levels, with the theoretical curves consistently lying above the experimental results and showing a far steeper stress dependence than is shown by the experimental trends, i.e., higher stress levels are required experimentally to reach similar craze velocities predicted by the model. This is the same effect exhibited by the

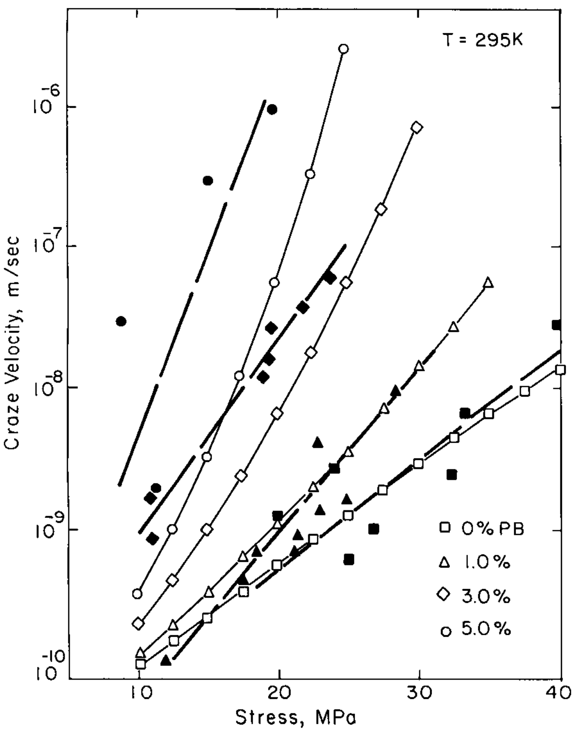

Figure 15 Calculated stress dependence of craze front velocity at 295K for the diluent PB used by Spiegelberg et al.[8], (with 71% 1,4 content) for 4 different levels of volume fraction of diluent. Experimental points are shown with filled symbols. Theoretical curves of narrower line width are identified with open symbols.

departures between the experimentally observed craze-flow stresses in comparison with those calculated from the model. The explanation of the effect is the same, that the diluent coverage of the craze plane and the autocatalytic plasticization is unable to keep-up with demands of the propagating deformation fronts at the base regions of the craze tufts.

For the results shown in Figure 16 representing behavior at 253K, the agreement required for the homo-PS necessitated an adjustment in the craze-dart angle ω to an almost unacceptable level of 0.314 for the same mean craze spacing $L_o = 2 \times 10^{-6}$m in the strain rate model from which the match was arranged. Clearly, if L_o is allowed to decrease, as is likely be the case, the craze-tip angle in the model could be less. Nevertheless, these changes in the model parameters do not, on the whole, produce better agreement between the model and the full range of experimental measurements. Thus, the conclusion remains that the diluent-plasticization effect has fundamental limitations resulting from the break-down of either the diluent spreading and/or the autocatalytic effect of plasticization.

RESULTS AND DISCUSSION

Conditions for Cut-off of Plasticizing Actions of Diluent

In the craze-flow stress model discussed in this article it was assumed that the Case II sorption front, under the accelerating action of the craze-flow stress, precedes, the intense drawing zone at the craze borders. This will cease to be so at low temperatures and high strain rates where the Case II sorption front velocity V will fall below the craze border velocity c_d, i.e.,

$$V < c_d. \tag{42}$$

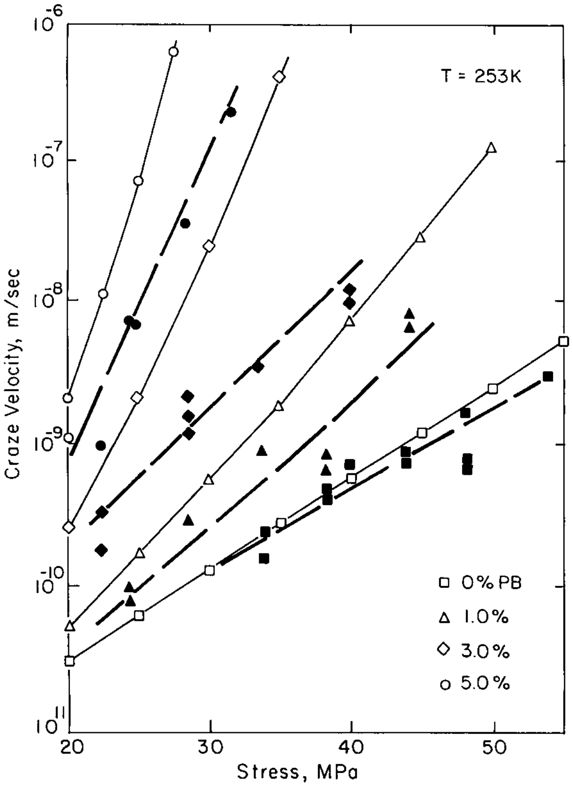

Figure 16 Calculated stress dependence of craze front velocity at 253K for the diluent PB used by Spiegelberg et al.[8], (with 71% 1,4 content) for 4 different levels of volume fraction of diluent. Experimental points are shown with filled symbols. Theoretical curves of narrower line width are identified with open symbols.

From Eq.(24) we have an expression for the craze border velocity as,

$$c_d = \frac{d}{\beta(\lambda_n - 1)}\,\dot{\epsilon}_e^p = \frac{C}{\beta\hat{Y}_o(\lambda - 1)}\left(\frac{\sigma_e}{\hat{Y}_o}\right)\dot{\epsilon}_e^p \quad (43)$$

where β is a concentration factor as defined previously having a magnitude of about 3 and $\dot{\epsilon}_e^p$ is the local equivalent plastic-strain rate at the countour (3) of Figure 12 and C = 2.5 × 10^{-7} MPa-m is the factor that relates the craze-tuft diameter to the craze-flow stress.[22] The dependence of $\dot{\epsilon}_e^p$ on equivalent stress σ_e is given by the mechanism-inspired expression of Argon and Bessonov,[22]

$$\dot{\epsilon}_e^p = \dot{\epsilon}_{AB}\exp\left[-\frac{B}{RT}\left(1 - \left(\frac{\sigma_e}{\hat{Y}_o}\right)^{5/6}\right)\right]. \quad (44)$$

While this expression has the proper mechanistic form of temperature and stress dependence, it is less convenient than a power-law representation of it that can be given as:

$$\dot{\epsilon}_e^p = \dot{\epsilon}_o(T)\left(\frac{\sigma_e}{\hat{Y}_o}\right)^m \quad (45)$$

where now both $\dot{\epsilon}_o(T)$ and the exponent m must be temperature dependent. For PS at room temperature $\dot{\epsilon}_o(T) = 6.5\ \mathrm{sec}^{-1}$ and $m = 7.68$. The term $\hat{Y}_o$ as defined previously in this article for PS at room temperature is 238MPa. In Eq.(45) σ_e, the local equivalent stress, is very close to the craze-flow stress σ_c as was also demonstrated previously. Under the action of the autocatalytic-plasticization effect $\hat{Y}_o \rightarrow \hat{Y}_o\exp(-m_p\varphi_e)$, where m_p, the plasticization factor has the value given in Table 1 for the appropriate diluent and φ_e is the diluent concentration given by Eq.(30) and listed in Table 1 for $f = 0.03$, the overall diluent concentration. We take $\lambda_n = 5$ as characteristic of the extension ratio of craze tufts.

For the Case II sorption front velocity we introduce a form that has resulted from a new theoretical model[17] that rectifies the well established deficiencies of the Thomas and Windle model with its linear viscous response.[16] Incorporating the substantial sorption-accelerating effect of an out-of-plane tensile stress[15,17] the required expression becomes,

$$V = V_o\left[\frac{4\mu}{\hat{Y}_o B'\varphi_e}\left[\frac{\sigma_e}{\hat{Y}_o} + \frac{B'\varphi_e}{2}\right]^m \exp(m m_p \varphi_e/2)\right]^{1/2} \quad (46)$$

where

$$V_o = \sqrt{D(T)\dot{\epsilon}_o(T)}, \quad (47a)$$

$$B' = \frac{6\epsilon_s\mu}{\hat{Y}_o}\left(\frac{1+\nu}{1-\nu}\right). \quad (47b)$$

In Eq.(47b) ϵ_s is a molecular volumetric size-misfit parameter of the sorbed diluent in the polymer, which is the principal cause of the plastic ejection of the swollen pressurized polymer in the Fickian precursor of the Case II sorption front.[17] Other quantities in Eqs.(46) and (47a) have been defined previously where, $D(T)$ is the diffusion constant of the diluent in the glassy polymer, in the Fickian precursor.

Restating the cut-off condition as

$$V^2 < c_d^2, \quad (47c)$$

we obtain after some simplification the condition,

$$D(T) < \dot{\epsilon}_o(T)\left(\frac{3}{2}\frac{\epsilon_s\varphi_e(1+\nu)}{(1-\nu)}\right)\left(\frac{\left(\frac{\sigma_c}{\hat{Y}_o}\right)^{2(m-1)/m}}{\frac{\sigma_c}{\hat{Y}_o} + \frac{B'\varphi_e}{2}}\right)^m \times \left(\frac{C}{3\hat{Y}_o(\lambda_n - 1)}\right)^2 \exp\left(\frac{7}{2}m_p m\varphi_e\right). \quad (48)$$

To test the utility of this condition we consider the specific diluent in the Spiegelberg experiments, i.e., PB − 3K with 71% of 1,4 isomer for which $m_p = 2.76$, $\varphi_e = 0.1581$ (for $f = 0.03$), $\nu = 0.3$, $\lambda_n = 5$, $\hat{Y}_o = 238$ Mpa, $\dot{\epsilon}_o(T) = 6.5\ \mathrm{sec}^{-1}$, $m = 7.68$, $C = 2.5 \times 10^{-7}$ MPa − m, $\mu = 1250$ MPa and the all important misfit parameter $\epsilon_s = 5.9 \times 10^{-3}$, fitted to the experiments of Kramer and co-workers, as described in detail in the full version of the new Case II sorption theory referred to above.[17] With these insertions based on the room temperature values of the various factors, we determine the cut-off condition to be,

$$D(T) = 4.98 \times 10^{-20}\ \mathrm{cm^2/sec}. \quad (49)$$

Nealey et al.[13] measured the diffusion constant of PB-3K (85% 1,4) in high molecular weight PS (M_w

= 350 and M_n = 170Kg/mole). A best fit to the temperature dependence of the measurements gave a relationship for the diffusion constant of:

$$D(T) = D_o \exp\left(-\frac{Q_D}{RT}\right) \tag{50}$$

with Q_D = 99 kcal/mole and $D_o = 8.40 \times 10^{43}$ cm^2/sec for measurements above the T_g of PS. Assuming that the relation of Eq.(50) might hold also below T_g, we consider the estimate for the cut-off condition given in Eq.(49) and use the expression of Eq.(50) to determine a cut-off temperature for the diluent-plasticization effect. For this we find $T_{\text{cut-off}}$ = 341K. However, the experimental results presented previously suggests that the cut-off temperature must be closer to 260K. From this discrepancy we must conclude that the effective Fickian diffusion constant must have been far higher at room temperature, suggesting that under the condition of active plastic deformation the activation energy for diluent diffusion must have been considerably lower than what was measured in the static experiments of Nealey et al..[13] While there is considerable room for substantial inaccuracies in the above estimates we consider this finding to be yet another demonstration of the autocatalytic nature of the diluent effects at the craze border where active-plastic flow at the base of craze tufts results in a dilated (flow state) in which diluent diffusion must be strongly enhanced.

Evaluation of the Potential of the Diluent-Induced Plasticization

The new experiments of Qin et al.[9] have demonstrated that the diluent-induced toughening mechanism discovered by Gebizlioglu et al.,[5] while extremely attractive in the conventional tensile deformation range, has important limitations at low temperatures and high strain rates, and with more viscous diluents which also have poorer sorption characteristics. Clearly, the diluent-toughening mechanism does not have the capability of providing toughness in the impact ranges of strain rate, even with the incorporation of a small fraction of craze initiating compliant particles, as has been developed by Qin et al..[25] The inadequacy of the mechanism for impact modification has been demonstrated earlier by Piorkowska et al..[26] In the present communication we have considered the new findings of Qin et al.[9] together with the results of the craze-plasticity studies of Spiegelberg et al.[7,8] in the framework of a new model of the crazing process. This has permitted a better assesment of the extremely complex and autocatalytic nature of the toughening mechanism acting in a very thin border region of thickening crazes. The new model incorporates all the known effects of stress, temperature, and diluent character and produces a useful semiquantitative insight into the complex processes. In the extreme ranges where the model fails, we have demonstrated that this results from a break down of the autocatalytic-plasticization effects.

The research was supported in its earlier form by NSF/MRL through the Center for Materials Science and Engineering (CMSE) at MIT under Grant DMR-90-22933 and more recently by the MRSEC Program of the NSF, again through the CMSE under Grant DMR-94-00334. The author is grateful to Prof. R.E. Cohen for many comments on the developments in this theoretical model.

LIST OF SYMBOLS

B	scale factor for activation free energy for strain rate in the plastic flow model of Argon-Bessonov
C	$(= \sigma_c \times d)$
$D(T)$	diffusion constant of diluent in PS
L_o	average spacing of active crazes in craze plasticity
R	craze tuft radius (Eqns. 22–24)
$R(t)$	radius of spreading diluent droplet (Eqns. 1–3)
R_o	initial radius of spreading diluent droplet
R	universal gas constant, when associated with T
$\hat{Y}_o$	athermal tensile plastic resistance in Argon-Bessonov model of polymer plasticity
V	average volume of diluent pool
V	velocity of Case-II sorption front at craze border (Eqn. 42)
a	average diameter of diluent pool
b	craze opening displacement at root of craze tip dart
c_d	translational velocity of craze tuft border
c	area fraction of propagating craze front wetted by diluent

d	diameter of craze tuft
f	volume fraction of diluent pools in polymer
h	length of craze tuft
$h(t)$	height of diluent droplet (Appendix I)
h_o	initial height of diluent droplet (Appendix I)
m	stress exponent in phenomonological strain rate expression
m_p	plasticization factor
n	number density per unit area of intercepted diluent pools on craze plane
r	radial coordinate
t	time
t_{oc}	terminal time for diluent spreading by a capillary mechanism
t_{og}	terminal time for diluent spreading by a gravitational mechanism
u_r	radial displacement
u_z	axial displacement
υ_c	craze front velocity
υ_d	drawing velocity of craze tuft
x	length coordinate
z	axial coordinate
$\Lambda(t)$	wetting length of spreading diluent slick at craze front
χ_B	surface free energy of PB
χ_S	surface free energy of PS
χ_{SB}	interface energy between PS/PB
$\dot{\delta}$	craze thickening rate
ϵ_s	misfit parameter of diluent molecule in PS
$\dot{\epsilon}_{AB}$	pre-exponential factor for plastic strain rate in the Argon-Bessonov model of polymer plasticity
$\dot{\epsilon}_c$	craze strain rate
$\dot{\epsilon}_o$	elongation rate (in Eqn. 23) ($\approx \dot{\epsilon}_e^p$)
$\dot{\epsilon}_o(T)$	phenomenological strain rate factor (in Eqn. 45)
$\dot{\epsilon}_e^p$	effective (equivalent) plastic strain rate
φ_e	volume fraction of sorbed diluent in active craze border
λ'	extension ratio in active drawing zone at base of craze tufts
λ_n	natural draw ratio of craze tuft
μ	shear modulus
ν	Poisson's ratio
ω	average craze tip angle
ρ	active craze front length per unit volume
σ_c	craze flow stress
τ	total time a spreading diluent slick maintains contact with advancing craze front
τ_f	frictional shear traction
η	extensional flow viscosity

APPENDIX I. SPREADING OF PB DILUENT ON CRAZE SURFACES

As depicted in Figures 3a and 3b we consider the lateral spreading of a PB diluent slug, first under the effect of gravity and then under capillary driving forces. Both analyses are of an approximate nature and must be viewed as merely useful for providing dimensionally correct, scalable forms.

Gravitational Spreading

Here we consider no wetting, either in accelerating or retarding the spreading process of the cylindrical slug of initial radius R_o and initial height h_o, having a volume $V = \pi R^2 h$ = constant at all times.

The vertical strain rate $\dot{\epsilon}_{zz}$ under the action of gravity is,

$$\dot{\epsilon}_{zz} = -\frac{1}{h}\frac{dh}{dt} = \frac{1}{\eta}\rho g h, \tag{AI-1}$$

where η is the extensional viscosity of the diluent and ρ its density. Direct integration gives for the current radius $R(t)$ at any given time t,

$$R(t) = R_o\sqrt{1 + t/t_{og}} \tag{AI-2}$$

where $t_{og} = \eta/h_o\rho g$.

In the experiments of Spiegelberg et al.[7] R_o was approximately 1mm and $h_o \approx R_o$ and the extensional viscosity at room temperature of the diluent around $\eta \approx$ 20Pa-s which gives t_{og} roughly as 20 sec.

Capillary Spreading

The diluent spreading on craze borders will be under the action of capillary driving forces as indicated in Figure 3c. The spreading diluent must satisfy equilibrium,

$$\frac{\partial \sigma_{rr}}{\partial r} + \frac{\sigma_{rr} - \sigma_{\theta\theta}}{r} - \frac{\partial \sigma_{zr}}{\partial z} = 0. \tag{AI-3}$$

We incorporate frictional traction by introducing a formal substitution for the last term, i.e.,

$$\frac{\partial \sigma_{zr}}{\partial z} \rightarrow \frac{\tau_f}{h}. \tag{AI-4}$$

We proceed by an upper bound analysis satisfying primarily kinematic requirements and dissipation rates. We start with a velocity field of,

$$\dot{u}_r = \frac{r}{R}\,v_o, \qquad \dot{u}_z = -\,2\,\frac{z_o}{R}\,v_o \quad \text{(AI-5a, b)}$$

Where $v_o = \dot{R}$ at the border of the slug. From conservation of volume of diluent, considering the slug to be thin and maintaining its cylindrical shape we have,

$$\dot{h} = -\,2\,\frac{h}{R}\,v_o. \qquad \text{(AI-5c)}$$

Thus, purely by kinematics we have,

$$\dot{\epsilon}_{rr} = \frac{\partial \dot{u}_r}{\partial r} = \frac{v_o}{R} \qquad \text{(AI-6a)}$$

$$\dot{\epsilon}_{zz} = \frac{\partial \dot{u}_z}{\partial z} = \frac{\dot{h}}{h} = -\,\frac{2v_o}{R} \qquad \text{(AI-6b)}$$

$$\dot{\epsilon}_{\theta\theta} = \frac{\dot{u}_r}{r} = \frac{v_o}{R}\,. \qquad \text{(AI-6c)}$$

Where the above give an equivalent strain rate $\dot{\epsilon}_e$ as,

$$\dot{\epsilon}_e = \left\{\frac{2}{9}\left[(\dot{\epsilon}_{rr} - \dot{\epsilon}_{\theta\theta})^2 + (\dot{\epsilon}_{\theta\theta} - \dot{\epsilon}_{zz})^2 + (\dot{\epsilon}_{zz} - \dot{\epsilon}_{rr})^2\right] + \frac{\dot{\gamma}_{rz}^2}{3}\right\}^{1/2} \qquad \text{(AI-7)}$$

where we take,

$$\dot{\gamma}_{rz} = \frac{v_o}{h}\,\frac{r}{R}\,. \qquad \text{(AI-8)}$$

This gives,

$$\dot{\epsilon}_e = \frac{v_o}{R}\,\sqrt{1 + \left(\frac{r}{h}\right)^2}\,. \qquad \text{(AI-9)}$$

But since over much of the range layer $\gg 1.0$ we have,

$$\dot{\epsilon}_e \cong \frac{v_o r}{Rh}\,. \qquad \text{(AI-10)}$$

With these, the internal dissipation rate $\dot{W}$ can be stated as,

$$\dot{W} = \int \tau\dot{\epsilon}_e dV = \int_o^R \eta\dot{\epsilon}_e^2 2\pi r h dr = \frac{\pi}{2}\,\eta\,\frac{R^2 v_o^2}{h}\,. \qquad \text{(AI-11)}$$

By the upper bound statement this must relate to the external driving force which we take as the radial stress governed by capillary conditions, i.e.,

$$\sigma_{rr} = (\chi_S - (\chi_B + \chi_{SB}))/h, \qquad \text{(AI-12)}$$

where χ_S and χ_B are the surface energies of PS and PB diluent and χ_{SB} as the interface energy between the two. Since,

$$\dot{W} = 2\pi R h v_o \sigma_{rr}, \qquad \text{(AI-13)}$$

we have the spreading front velocity $v_o = \dot{R}$ as,

$$v_o = \dot{R} = \frac{4h}{\eta R}\,A \qquad \text{(AI-14)}$$

where

$$A = \chi_S - (\chi_B + \chi_{SB}). \qquad \text{(AI-15)}$$

Through conservation of diluent volume V, we have finally,

$$\dot{R} = \frac{4VA}{\pi\eta}\,\frac{1}{R^3}\,. \qquad \text{(AI-16)}$$

Direct integration gives,

$$R(t) = R_o\left(1 + \frac{t}{t_{oc}}\right)^{1/4}, \qquad \text{(AI-17)}$$

where

$$t_{oc} = \frac{\pi\eta R_o^4}{16VA}\,. \qquad \text{(AI-18)}$$

If the diluent appears in the polymer in the form of spherical pools of diameter a then $V = \pi a^3/6$ and by stereology of sampling $R_o \cong \pi a/8$. This gives,

$$t_{oc} = 8.92 \times 10^{-3}\eta a/A \qquad \text{(AI-19)}$$

APPENDIX II. STEADY-STATE FRACTION OF CRAZE FRONT COVERED BY DILUENT SLICKS CONTACTED BY A CRAZE

Consider a craze front advancing with a velocity v_c, tapping into a diluent pool at time $t = 0$. At time t the spreading diluent slick of radius *R(t)* on the craze surface covers a length Λ of the craze front, as shown in Figure 5,

$$\Lambda(t) = \sqrt{(2R(t))^2 - (2v_c t)^2}. \qquad \text{(AII-1)}$$

Assuming that there is no lateral capillary interaction of the diluent slick with the craze front, the total time τ that a spreading slick of initial radius R_o makes contact with the advancing craze front can be found from the condition,

$$R(\tau) = v_c\tau. \qquad \text{(AII-2)}$$

With the use of Eq.(AI-17) we can write the equation for the time τ as,

$$\frac{v_c t}{R_o}\left(\frac{\tau}{t_{oc}}\right)^4 - \left(\frac{\tau}{t_{oc}}\right) - 1 = 0. \qquad \text{(AII-3)}$$

If the average diluent pool has a diameter a and the total diluent volume fraction is f, the number density N on the craze plane should be,

$$N = \frac{64f}{\pi^3 a^2} \qquad \text{(AII-4)}$$

Referring to Figure 6, the number dn per unit length of intercepted diluent pools in a strip dx is,

$$dn = Ndx = \frac{64f}{\pi^3 a^2}\,dx. \qquad \text{(AII-5)}$$

The contribution to the diluent coverage of the craze front line of pools contained by the strip of width dx currently at distance x behind the front is,

$$\Lambda(x)dn = \Lambda(x)\,\frac{64f}{\pi^3 a^2}\,dx \qquad \text{(AII-6)}$$

where

$$\Lambda(x) = \sqrt{(2R_o)^2\left(1 + \frac{x}{v_c t_{oc}}\right)^{1/2} - (2x)^2}, \qquad \text{(AII-7)}$$

and is obtained from Eq. AII-1 with a substitution of $x = v_c t$ Then, the total line length of craze front covered by diluent per unit length of craze front should be, c, the fraction of the craze front coverage, as,

$$c = \int_o^{x=R(\tau)} \Lambda(x)\,\frac{64f}{\pi^3 a^2}\,dx. \qquad \text{(AII-8)}$$

The time t where contact is lost between a spreading slick (initiated at time $t = 0$) and the craze front is the solution of equation (AII-3), which can also be restated as an equation for the final radius R_f of the slick where contact is lost by replacing $R_f = v_c\tau$. *This gives,*

$$\left(\frac{R_f}{R_o}\right)^4 - \left(\frac{R_f}{R_o}\right)\left(\frac{R_o}{v_c t_{oc}}\right) - 1 = 0. \qquad \text{(AII-9)}$$

We now note that $R_o = \pi a/8$, $t_{oc} = 8.9 \times 10^{-3}\eta a/A$ (from (AI-19) with $\eta \approx 10$ Pa-s, A $\approx 0(10^{-2})\ J/m^2$, and taking as a typical craze velocity of $v_c = 10^{-8}$ m/sec, the factor $R_o/v_c t_{oc}$ is of order 4.4×10^6. Since $R_f/R_o > 1.0$, the last term in Eq.(AII-9) can be neglected giving,

$$\frac{R_f}{R_o} \cong \left(\frac{R_o}{v_c t_{oc}}\right)^{1/3}. \qquad \text{(AII-10)}$$

Then, the steady state diluent coverage of the advancing craze front becomes,

$$c = \frac{2}{\pi} f \int_o^{\zeta=\zeta_c} \sqrt{(1 + \zeta_c^3\zeta)^{1/2} - \zeta^2}\,d\zeta, \qquad \text{(AII-11)}$$

where we have made the following abreviations, $\zeta = x/R_o$ and $\zeta^3{}_c = R_o/v_c t_{oc}$. With a further normalization of $\xi = \zeta/\zeta_c$ we have,

$$c = \frac{2}{\pi} f\zeta_c \int_o^1 \sqrt{(1 + \zeta_c^4\xi)^{1/2} - \zeta_c^2\xi^2}\,d\xi \qquad \text{(AII-12)}$$

Since $\zeta_c \gg 1.0$, as demonstrated above, the expression can be simplified further as,

$$c = \frac{2\beta}{\pi} f \zeta_c^2 \qquad \text{(AII-13)}$$

where

$$\beta = \int_o^1 \sqrt{\xi^{1/2} - \xi^2}\, d\xi = 0.561. \qquad \text{(AII-14)}$$

Restoring terms to their actual dimensions, we obtain with the use of Eq.(AI-18),

$$c = \frac{25}{\pi} \beta f \left(\frac{A}{v_c \eta} \right)^{2/3}. \qquad \text{(AII-15)}$$

Proceeding further, the craze velocity can be related to the craze strain rate $\dot{\epsilon}_c$ through Eqs. (18–20) to give,

$$v_c = \frac{\dot{\epsilon}_c}{b\rho} \qquad \text{(AII-16)}$$

giving,

$$c = \frac{25}{\pi} \beta f \left(\frac{Ab\rho}{\dot{\epsilon}_c \eta} \right)^{2/3} \qquad \text{(AII-17)}$$

where $b\rho$ has typically a magnitude of around $2.5 \times 10^4 \mathrm{m}^{-1}$ for craze plasticity. From Eq.(AII-17) for $A = 10^{-2}/m, \eta = 10\mathrm{Pa\text{-}s}, f = 0.03$, we can determine the cut-off strain rate where the craze front coverage of diluent would become discontinuous i.e. $c < 1.0$ as,

$$\dot{\epsilon}_{\text{cut-off}} = \frac{A(b\rho)}{\eta} \left(\frac{25\beta f}{\pi} \right)^{3/2} \qquad \text{(AII-18)}$$

which gives for the above values a strain rate of 1.26 sec^{-1}.

REFERENCES AND NOTES

1. Kramer, E. J. in Advances in Polymer Science, Vol. 52/53, Kausch, H. H., Ed.; Springer, Berlin, 1983, pp. 1–56.
2. Kramer, E. J.; Berger, L. L. in Advances in Polymer Science, Vol.91/92, Kausch, H. H., Ed.; Springer, Berlin, 1990, pp.1–8.
3. Argon, A. S.; Cohen, R. E.; Gebizlioglu, O. S.; Schwier, C. E.; in Advances in Polymer Science, Vol. 52/53, Kausch, H., Ed.; Springer, Berlin,1983, pp. 275–334.
4. Argon, A. S.; Cohen, R. E. in Advances in Polymer Science, Vol. 91/92, Kausch, H. H., Ed.; Springer, Berlin, pp. 301–351.
5. Gebizlioglu, O. S.; Beckham, H. W.; Argon, A. S.; Cohen, R. E.; Brown, H. R. Macromolecules 1990, 23, 3968.
6. Argon, A. S.; Cohen, R. E.; Gebizlioglu, O. S.; Brown, H. R.; Kramer, E. J. Macromolecules 1990, 23, 3975.
7. Spiegelberg, S. H.; Argon, A. S.; Cohen, R. E. J Appl Polym Sci 1993, 48, 85.
8. Spiegelberg, S. H.; Argon, A. S.; Cohen, R. E. J Appl Polym Sci 1994, 53, 1251.
9. Qin, J.; Argon, A. S.; Cohen, R. E. J Appl Polym Sci (binary blends) in press.
10. Gebizlioglu, O. S.; Argon, A. S.; Cohen, R. E. Polymer 1985, 26, 519.
11. Gebizlioglu, O. S.; Argon, A. S.; Cohen, R. E. Polymer 1985, 26, 529.
12. Brown, H. R.; Argon, A. S.; Cohen, R. E.; Gebizlioglu, O. S.; Kramer, E. J. Macromolecules 1989, 22, 1002.
13. Nealey, P. F.; Cohen, R. E.; Argon, A. S. Macromolecules 1993, 26, 1287.
14. Nealey, P. F.; Cohen, R. E.; Argon, A. S. Polymer 1995, 36, 3687.
15. Brown, H. R. J Polym Sci Polym Phys Ed 1989, 27, 1273.
16. Thomas, N. L.; Windle, A. H. Polymer 1982, 23, 529.
17. Argon, A. S.; Cohen, R. E.; Patel, A. Polymer submitted for publication.
18. Gall, T. P.; Lasky, R. C.; Kramer, E. J. Polymer 1990, 31, 1491.
19. Harmon, J. P.; Lee, S.; Li, J. C. M. J Polym Sci Polym Chem Ed 1987, 25, 3215.
20. Zhou, Q.-Y.; Argon, A. S.; Cohen, R. E. Polymer submitted for publication.
21. Chemical Engineers Handbook, Perry, J. H., Ed.; McGraw-Hill, New York, 1941, p. 796.
22. Hutchinson, J. W.; Neale, K. W. J Mech Physics of Solids 1983, 31, 405.
23. Boyce, M. C.; Montagut, E. L.; Argon, A. S. Polymer Eng Sci 1992, 32, 1073.
24. Argon, A. S.; Bessonov, M. I. Phil Mag 1977, 35, 917.
25. Qin, J.; Argon, A. S.; Cohen, R. E. J Appl Polym Sci (ternary blends) in press.
26. Piorkowska, E.; Argon, A. S.; Cohen, R. E. Polymer 1993, 34, 4435.